Interleaving and switching pattern modulation to conducted EMI reduction

J. Mon, D. González, J. Gago, J. Balcells, P. Bogónez

Departament d'Enginyeria Electrònica. Universitat Politècnica de Catalunya.
Campus de Terrassa. 08222 Terrassa, Spain. juan.mon@upc.edu

Abstract: This paper explores new techniques to reduce the conducted EMI generated by switched power converters operating in multiconverter arrangement. These techniques are based in the combined application of interleaving and the modulation of some characteristics of the switching patterns. The effectiveness of such methods in terms of EMI reduction is theoreticaly developed and experimentally validated in a four channel parallel buck converter operating in closed loop. The technique that provides the best attenuation results is identified. Finally, undesired side-effects produced by these techniques, such as an increase in the output voltage ripple, are evaluated.

Keywords: EMC, EMI, Frequency modulation, Interleaving, Modulation.

1. INTRODUCTION

Power converters are normally operated with constant frequency in hard switching regime using Pulse Width Modulation techniques. In a general way, the modulator is the block that generates the switching patterns from the control signal generated by the converter controller. Therefore, it is the block responsible of the main source of EMI. Since Spread Spectrum Modulation was introduced as EMI reduction technique in switched power converters, a lot of works have been published developing this idea [1-7]. At present, it is a well established technique and a worthy alternative to the traditional filtering methods such as the bulky EMI filters or snubber networks in terms of attenuation, cost and simplicity of application. However, the application of modulation based techniques on multiconverter arrangement has not been deeply explored yet.

Spread Spectrum Modulation in single converter consists of modulating the switching period, T_k, around a central value, T_c, according to a given modulation function. The characteristics of the modulation function will affect the resulting conducted EMI spectrum. The modulation function can be random [2,7] or deterministic [4-6]. The modulation function in random modulations is generally expressed as a density of probability function. In general terms, it has been shown that this kind of modulations leads to a high content in low frequency harmonics [2].

Regarding periodic modulations, Fig. 1 shows a triangular modulation function, $V_m(t)$, and the resulting switching pattern as well. This modulation profile

produces an energy spread of the initial harmonics under a flat envelope and it has been successfully applied to DC/DC and AC/DC converters in previous works [3]. The relationship between parameters of $V_m(t)$ and the resulting spectrum characteristics can be found in [4].
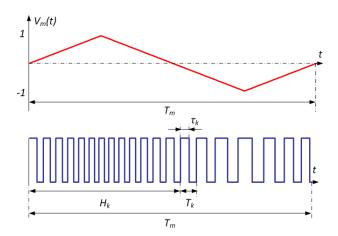

Figure 1: Spread Spectrum Modulation with periodic modulation profile

The instantaneous switching period can be approximated to (1),

$$T_k = T_c + \Delta T_k \approx \frac{1}{f_c + \Delta f_c V_m\left(H_k\right)} \qquad (1)$$

where f_c is the central switching frequency, Δf_c is the maximum frequency deviation and H_k is the starting time of the k-th switching cycle, that is given by (2).

$$H_k = \begin{cases} 0 & k=1 \\ \sum_{j=1}^{k-1} T_j & k>1 \end{cases} \qquad (2)$$

On the other hand, interleaving is a well known and well established technique used in multiconverter arrangement. Its underlying principle is the time-shift among the switching patterns of the different converters. Consider a system of N converters operating at the same switching period, T_c, on which a time delay of T_c/N is introduced among the switching patterns [8]. From the point of view of disturbance generation, it is equivalent to a single converter operated at frequency Nf_c [9, 10]. Therefore, the output voltage/current ripple of the full system is reduced.

In this work, we explore the optimal combination of interleaving and periodic modulation techniques to be applied to modular power supplies systems with parallel topology in order to obtain the best conducted EMI attenuation [12-14]. We also pay attention to the undesired side-effects of such techniques on the converter performance [3, 11]. The experimental validation has been performed on four buck converters connected in parallel.

2. DESCRIPTION OF THE SWITCHING PATTERNS

There are several possibilities of combination interleaving and spread spectrum modulation in multiconverter arrangement. Fig. 2 represents a generic switching pattern for a multiconverter arrangement, where i notes each channel ($i=1,2,..,N$), α_i is the delay among switching patterns, $q_i(t)$, and $\varepsilon_{k,i}$ is the pulse position delay inside each switching cycle. Each switching pattern contains L switching cycles (3). Notice that each switching pattern has a period equal to the period of the modulation profile, T_m.

$$L = \frac{T_m}{T_c}, \; L \, integer > 0 \qquad (3)$$

Table I summarizes the characteristic of the three switching patterns considered in this paper: Constant Delay Frequency Modulation for Tm (CDFM-Tm), Constant Delay Frequency Modulation for Tc (CDFM-Tc) and Variable Delay Frequency Modulation (VDFM). In all cases, a modulation on the switching period is introduced according to a triangular modulation profile. On the other hand, the value of the duty cycle, D_c, is always established by the controller.

In order to evaluate the attenuation provided by the proposed modulations, a time domain description of the switching pattern is needed.
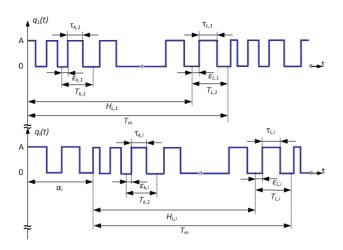

Figure 2: Generic switching patterns

TABLE I.   MODULATION PARAMETERS

Modulations	$\varepsilon_{k,i}$	$T_{k,i}$	$\tau_{k,i}$	α_i
CDFM-Tm	$0 \nabla i, k$	$T_k = T_c + \Delta T_k \nabla i$	$D_c T_k \nabla i$	$\frac{T_m}{N}(i-1)$
CDFM-Tc	$0 \nabla i, k$	$T_k = T_c + \Delta T_k \nabla i$	$D_c T_k \nabla i$	$\frac{T_c}{N}(i-1)$
VDFM	$\frac{T_{k,i}}{N}(i-1)$	$T_k = T_c + \Delta T_k \nabla i$	$D_c T_k \nabla i$	$0 \nabla i$

Considering that a switching pattern has a period equal to the modulation profile period, T_m, the time domain expression of each of them, $q_i(t)$, can be written as (4).

$$q_i(t) = \sum_{n=-\infty}^{\infty} C_{i,n} e^{\frac{-j2\pi n t}{T_m}} = C_{i,0} + 2\sum_{n=1}^{\infty} C_{i,n} e^{\frac{-j2\pi n t}{T_m}} \qquad (4)$$

where $C_{i,n}$ are the Fourier coefficients.

By calculating the Fourier coefficients, the switching pattern can be written as (5)

$$q_i(t) = \frac{A}{T_m} \sum_{k=1}^{L} \tau_{k,i} + \sum_{n=1}^{\infty} \left(\frac{A}{j\pi n} e^{\frac{-j2\pi n \alpha_i}{T_m}} \right.$$
$$\left. \times \sum_{k=1}^{L} \left[e^{\frac{-j2\pi n (\varepsilon_{k,i}+H_{k,i})}{T_m}} \left(1 - e^{\frac{-j2\pi n \tau_{k,i}}{T_m}} \right) \right] e^{\frac{-j2\pi n t}{T_m}} \right) \qquad (5)$$

where A is the amplitude of each switching pattern.

Finally, the equivalent source of noise, $s(t)$, for a multiconverter arrangement with N channels is determined by the addition of each particular pattern, $q_i(t)$, according to (6).

$$s(t) = \sum_{i=1}^{N} q_i(t) \qquad (6)$$

A. Constant Delay Tm with switching Frequency Modulation (CDFM-Tm)

The interleaving effect is obtained by introducing a constant delay α_i among the N switching patterns in addition to the switching period modulation. This α_i delay is determined by the period of the modulation profile, T_m. Considering the values of Table I and (7), the equivalent source of noise, in frequency domain, $S_{CDFM\text{-}Tm}(w)$, can be expressed by (8).

$$H_{k,i} = H_k \ \nabla i \qquad (7)$$

$$S_{CDFM-Tm}(w) = F\left\{\sum_{i=1}^{N} q_i(t)\right\} = NAD_c \partial(w) + \sum_{n=1}^{\infty}\left(\frac{A}{j\pi n}\right)$$

$$\times \left[\frac{1-e^{\frac{-j2\pi n}{L}}}{1-e^{\frac{-j2\pi n}{N}}}\right] \sum_{k=1}^{L}\left[e^{\frac{-j2\pi n H_k}{T_m}}\left(1-e^{\frac{-j2\pi n D_c T_k}{T_m}}\right)\right]\partial(w-nw_m)\right) \qquad (8)$$

$$= NAD_c \partial(w) + N\, E_{CDFM-Tm}(w)$$

$$\times \sum_{n=1}^{\infty}\left(\frac{A}{j\pi n}\sum_{k=1}^{L}\left[e^{\frac{-j2\pi n H_k}{T_m}}\left(1-e^{\frac{-j2\pi n D_c T_k}{T_m}}\right)\right]\partial(w-nw_m)\right)$$

where w_m is the modulation profile frequency (9).

$$w_m = 2\pi f_m = \frac{2\pi}{T_m} \qquad (9)$$

Notice that the absolute value of $E_{CDFM\text{-}Tm}(w)$ takes the values of (10).

$$\left|E_{CDFM-Tm}(w)\right| = \begin{cases} 0 & n = hN \\ 1 & n \neq hN \end{cases} \quad h=0,1,2,\ldots,\infty \quad (10)$$

Therefore, (8) can be written as (11).

$$S_{CDFM-Tm}(w) = \left\{\sum_{i=1}^{N} q_i(t)\right\} = NAD_c \partial(w) + \sum_{n=1}^{\infty}\left(\frac{A}{j\pi n}\right)$$

$$\times N\sum_{k=1}^{L}\left[e^{\frac{-j2\pi n H_k}{T_m}}\left(1-e^{\frac{-j2\pi n D_c T_k}{T_m}}\right)\right]\partial(w-nNw_m) \qquad (11)$$

In this case, the spectrum consists of components at frequencies nNf_m.

B. Constant Delay Tc with switching Frequency Modulation (CDFM-Tc)

In this modulation, the delay α_i among the switching patterns is calculated from the central value of switching cycle, T_c. The equivalent noise pattern in frequency domain, $S_{CDFM\text{-}Tc}(w)$, can be expressed according to (12).

$$S_{CDFM-Tc}(w) = F\left\{\sum_{i=1}^{N} q_i(t)\right\} = NAD_c \partial(w) + \sum_{n=1}^{\infty}\left(\frac{A}{j\pi n}\right)$$

$$\times \left[\frac{1-e^{\frac{-j2\pi n}{L}}}{1-e^{\frac{-j2\pi n}{NL}}}\right] \sum_{k=1}^{L}\left[e^{\frac{-j2\pi n H_k}{T_m}}\left(1-e^{\frac{-j2\pi n D_c T_k}{T_m}}\right)\right]\partial(w-nw_m)\right) \qquad (12)$$

$$= NAD_c \partial(w) + N\, E_{CDFM-Tc}(w)$$

$$\times \sum_{n=1}^{\infty}\left(\frac{A}{j\pi n}\sum_{k=1}^{L}\left[e^{\frac{-j2\pi n H_k}{T_m}}\left(1-e^{\frac{-j2\pi n D_c T_k}{T_m}}\right)\right]\partial(w-nw_m)\right)$$

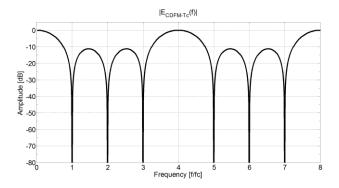The value of $|E_{CDFM\text{-}Tc}(w)|$ is shown in Fig. 3 for $N=4$.

Figure 3: Envelope of $|E_{CDFM\text{-}Tc}(f)|$ for $N=4$

From Fig. 3 harmonic cancellation is noticed at frequencies nf_c except those multiple of Nf_c. In comparison to CDFM-Tm, an additional attenuation is observed for all frequencies, except those multiple of Nf_c. Therefore, a better attenuation performance than CDFM-Tm is expected.

C. Variable Delay with switching Frequency Modulation (VDFM)

In VDFM there is any delay among switching patterns ($\alpha_i = 0$). In this case, a delay on each particular switching cycle, $\varepsilon_{k,i}$, is introduced according to Table I. The equivalent noise pattern in frequency domain, $S_{VDFM}(w)$, can be expressed according to (13).

$$S_{VDFM}(w) = F\left\{\sum_{i=1}^{N} q_i(t)\right\} = NAD_c \partial(w) + \sum_{n=1}^{\infty}\left(\frac{A}{j\pi n}\right)$$

$$\times \sum_{k=1}^{L}\left[e^{\frac{-j2\pi n H_k}{T_m}}\left(\frac{1-e^{\frac{-j2\pi n T_k}{T_m}}}{1-e^{\frac{-j2\pi n T_k}{NT_m}}}\right)\left(1-e^{\frac{-j2\pi n D_c T_k}{T_m}}\right)\right]\partial(w-nw_m)\right) \qquad (13)$$

The resulting spectrum of VDFM is equivalent to a single converter operated at Nf_c with spread spectrum frequency modulation.

3. EXPERIMENTAL RESULTS

Two kinds of measurements have been conducted. First of all, we performed conducted EMI measurements on the LISN and with a high frequency current clamp in order to separate propagation modes (Common and Differential Modes). On the other hand, we measured the output voltage ripple in order to evaluate undesired side effects. The experimental results have been obtained for a central switching frequency f_c=300 kHz, a triangular modulation profile (Fig. 1), $V_m(t)$, with a modulation frequency f_m=10 kHz and a maximum frequency deviation Δf_c= 60 kHz. The f_m parameter has been chosen considering the Resolution Bandwidth (RBW) of the EMI receptor [4].

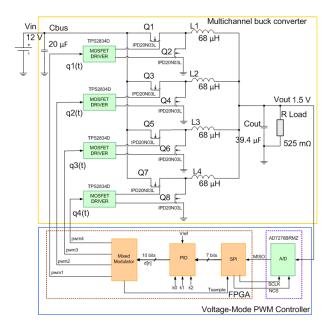Fig. 4 shows a diagram block of the experimental plant and the operating conditions.

Figure 4: Block diagram of the experimental plant.

A. EMI measurements

The experimental setup is schematically depicted in Fig. 5.

Fig. 6 shows the attenuation of conducted EMI up to 30 MHz obtained with CDFM-Tc, CDFM-Tm and VDFM respectively.
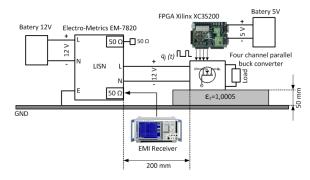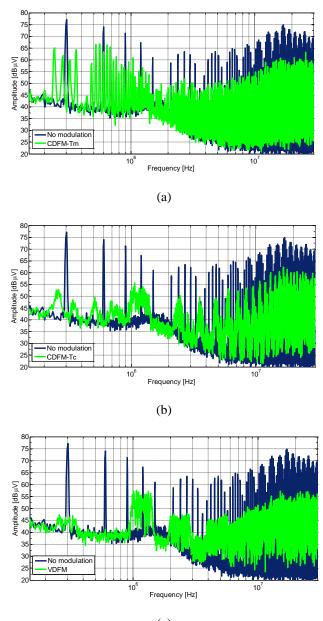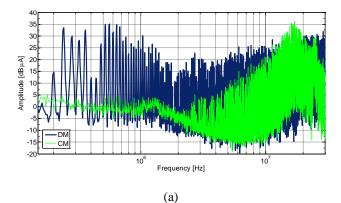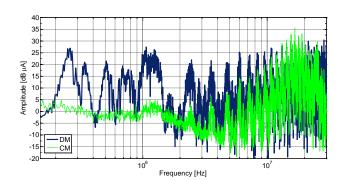

Figure 5: EMI measurement set-up

(a)

(b)

(c)

Figure 6: Attenuation performance: (a) CDFM-Tm, (b) CDFM-Tc, (c) VDFM

As it has been demonstrated in section 2, the CDFM-Tc and VDFM provide the best attenuation. The harmonic cancelation effect of CDFM-Tc that is predicted in Fig. 3 is clearly noticeable in Fig. 6(b). The best attenuation is given by VDFM. In the low frequency range (up to the 4th harmonic) the cancelation effect is clearly noticed. For higher frequencies, the combination of cancelation and energy spread effects provides an attenuation of almost 15dB in all the spectrum.

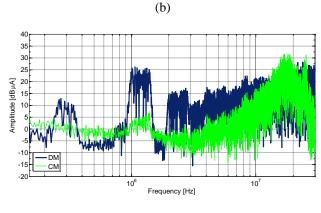Regarding propagation modes, Fig. 7 shows the common and differential modes for the three modulations proposed.

(a)

(b)

(c)

Figure 7: CM and DM current (a) CDFM-Tm, (b) CDFM-Tc, (c) VDFM

B. Output voltage ripple

Techniques based on spread spectrum can lead to undesired side effects on the converter performance. It has been demonstrated that power efficiency is not clearly affected [3]. The most noticeable effect will appear as an increase of the output voltage ripple [11]. The output voltage ripple without modulation neither interleaving is 11mV. Fig. 8 compares the output voltage ripple in all cases considered. The modulation frequency, f_m, is clearly reflected in the output voltage. This effect is less noticeable in CDFM-Tm due to the delay introduced among switching patterns.
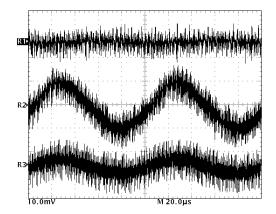

Figure 8: Output voltage ripple comparison: CDFM-Tm, CDFM-Tc and VDFM (R1: CDFMTm; R2: CDFM-Tc; R3:VDFM)

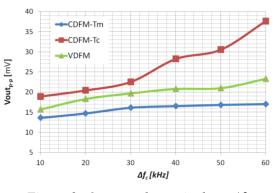The output voltage ripple as a function of Δfc appears in Fig. 9.

Figure 9: Output voltage ripple vs Δf_c

4. CONCLUSIONS

In this paper, three EMI suppression techniques that combine interleaving and spread spectrum modulation has been presented. The attenuation provided by such techniques were theoretically explored and practically validated in a four channels buck converter in parallel arrangement and operated in closed loop.

EMI attenuation obtained with these techniques has been measured on the full band B (150 kHz- 30 MHz) of conducted disturbances. As a reference to evaluate attenuation, converters were operated at constant frequency and without interleaving.

The VDFM is the technique that provides the best trade-off between attenuation and converter performance degradation in terms of output voltage ripple. CDFM-Tc shows similar attenuation but with worse results in terms of output voltage ripple.

5. ACKNOWLEDGMENT

6. REFERENCES

[1] Feng Lin and Chen, D.Y., "Reduction of Power Supply EMI Emission by Switching Frequency Modulation", *IEEE Trans. on Power Electronics*, vol. 9, n0. 1, pp. 132 – 137, January 1994.

[2] Tse, K.K., Henry Shu-Hung Chung, Ron Hui, S.Y. and So, H.C., "A comparative study of carrier-frequency modulation techniques for conducted EMI suppression in PWM converters", *IEEE Trans. on Industrial Electronics*, vol. 49, no. 3, pp. 618 – 627, June 2002.

[3] Gonzalez, D., Balcells, J., Santolaria, A., Le Bunetel, J-Ch., Gago, J., Magnon, D. and Brehaut, S., "Conducted EMI Reduction in Power Converters by Jeans of Periodic Switching Frequency Modulation", *IEEE Trans. on Power Electronics,* vol. 22, no. 6,pp. 2271–2281, November 2007.

[4] Balcells J., Santolaria A., Orlandi A., Gonzalez D. and Gago J., "EMI reduction in switched power converters using frequency Modulation techniques", *IEEE Trans. on Electromagnetic Compatibility*, vol. 47, no. 3, pp. 569 – 576, August 2005.

[5] Gonzalez, D., Bialasiewicz, J-T., Balcells, J. and Gago, J., "Wavelet-Based Performance Evaluation of Power Converters Operating With Modulated Switching Frequency", *IEEE Trans. on Industrial Electronics*, vol. 55, no. 8, pp. 3167 – 3176, August 2008.

[6] Barragan, L., Navarro, D., Acero, J., Urriza, I. and Burdío, J-M., "FPGA Implementation of a Switching Frequency Modulation Circuit for EMI Reduction in Resonant Inverters for Induction Heating Appliances", *IEEE Trans. on Industrial Electronics*, vol. 55, no. 1, pp. 11 – 20, January 2008.

[7] G. Dousoky, M. Shoyama, and T. Ninomiya, "FPGA-Based Spread-Spectrum Schemes for Conducted-Noise Mitigation in DC-DC Power Converters: Design, Implementation, and Experimental Investigation," *IEEE Trans. on Industrial Electronics*, vol. 58, no. 2, pp. 429 –435, February 2011.

[8] C. Chang and M. A. Knights, "Interleaving Technique in Distributed Power Conversion Systems," *EEE Trans. Circuits Syst. I*, vol. 42, no. 5, pp. 245–251, May 1995.

[9] Ozeri S., Shmilovitz D., Singer S. and Martinez-Salamero L., "The Mathematical Foundation of Distributed Interleaved Systems", *IEEE Trans. on Circuits and Systems--I:* vol. 54, no. 3, pp. 610-619, March 2007.

[10] P. Zumel, O. Garcia, J. A. Oliver, and J. A. Cobos, "Differential-Mode EMI Reduction in a Multiphase DCM Flyback Converter," *IEEE Trans. on Power Electronics*, vol. 24, no. 8, pp. 2013–2020, August 2009.Zumel 2009.

[11] A. Santolaria, "Effects of Switching Frequency Modulation on the Power Converter's Output Voltage," *IEEE Trans. on Industrial Electronics*, vol. 56, no. 7, pp. 2729–2737, July 2009.

[12] Mon, J., Gonzalez, D., Gago, J. and Balcells, J., "Combined application of interleaving and modulation techniques in multiconverter topology", *IEEE International Conference on Electronics, Circuits and Systems*, ICECS 2008, pp. 1087-1090.

[13] Mon, J., Gago, J., Gonzalez, D., Balcells, J., Fernandez, R. and Gil, I., "A new switching frequency modulation scheme for EMI reduction in multiconverter topology", *European Conference on Power Electronics and Applications*, EPE 2009, Barcelona, September 2009.

[14] J. Mon, D. Gonzalez, J. Gago, J. Balcells, R. Fernandez, and I. Gil., "Contribution to conducted EMI reduction in multiconverter topology", *In Proc. IECON'09*, pp. 4086 –4091, 2009.